Vol. 14, pp. 191–198 (2017)
doi: 10.2142/biophysico.14.0_191

Biophysics and Physicobiology

https://www.jstage.jst.go.jp/browse/biophysico/

Review Article

Structural differences in the bacterial flagellar motor among bacterial species

Hiroyuki Terashima[1], Akihiro Kawamoto[2], Yusuke V. Morimoto[3], Katsumi Imada[4] and Tohru Minamino[5]

[1]*Division of Biological Science, Graduate School of Science, Nagoya University, Nagoya, Aichi 464-8602, Japan*
[2]*Institute for Protein Research, Osaka University, Suita, Osaka 565-0871, Japan*
[3]*Department of Bioscience and Bioinformatics, Faculty of Computer Science and Systems Engineering, Kyushu Institute of Technology, Iizuka, Fukuoka 820-8502, Japan*
[4]*Department of Macromolecular Science, Graduate School of Science, Osaka University, Toyonaka, Osaka 560-0043, Japan*
[5]*Graduate School of Frontier Biosciences, Osaka University, Suita, Osaka 565-0871, Japan*

Recieved October 23, 2017; accepted November 19, 2017

The bacterial flagellum is a supramolecular motility machine consisting of the basal body as a rotary motor, the hook as a universal joint, and the filament as a helical propeller. Intact structures of the bacterial flagella have been observed for different bacterial species by electron cryotomography and subtomogram averaging. The core structures of the basal body consisting of the C ring, the MS ring, the rod and the protein export apparatus, and their organization are well conserved, but novel and divergent structures have also been visualized to surround the conserved structure of the basal body. This suggests that the flagellar motors have adapted to function in various environments where bacteria live and survive. In this review, we will summarize our current findings on the divergent structures of the bacterial flagellar motor.

Key words: bacterial flagellum, electron cryotomography, motility, rotary motor, structural diversity

Corresponding author: Tohru Minamino, Graduate School of Frontier Biosciences, Osaka University, 1-3 Yamadaoka, Suita, Osaka 565-0871, Japan.
e-mail: tohru@fbs.osaka-u.ac.jp

A huge variety of bacteria live on our planet. Bacteria adapt and evolve in their living environment. Many bacteria swim in liquid environments and move on solid surfaces towards more favorable conditions and escape from undesirable ones for their survival. The bacterial flagellum is a supramolecular motility machine consisting of about 30 different proteins. These component proteins are highly conserved among bacterial species. The bacterial flagellum can be divided into at least three parts: the basal body, the hook and the filament. The basal body is embedded within the cell membranes and acts as a rotary motor. The hook and filament extend outwards in the cell exterior. The filament works as a helical propeller. The hook connects the basal body and filament and functions as a universal joint to smoothly transmit torque produced by the motor to the filament [1–4].

The flagellar basal body of *Escherichia coli* and *Salmonella enterica* serovar Typhimurium (hereafter referred to as *Salmonella*) consists of the C ring (FliG, FliM, FliN), the MS ring (FliF), the P ring (FlgI), the L ring (FlgH), the rod (FliE, FlgB, FlgC, FlgF, FlgG) and the protein export apparatus (FlhA, FlhB, FliH, FliI, FliJ, FliP, FliQ, FliR). In addition, a dozen stator units (MotA, MotB) surround the basal

◀ ***Significance*** ▶

The bacterial flagellum is a supramolecular motility machine consisting of a rotary motor, a universal joint and a helical propeller. Component proteins of the flagellar motor are highly conserved among bacterial species. Recent structural analyses of intact flagellar motors derived from different bacterial species by electron cryotomography and subtomogram averaging have shown that novel and divergent structures surround the conserved structure in different species, suggesting that the flagellar motors have adapted to function in their living environment. In this review article, we will describe the conserved structure of the flagellar motor and its structural diversity.

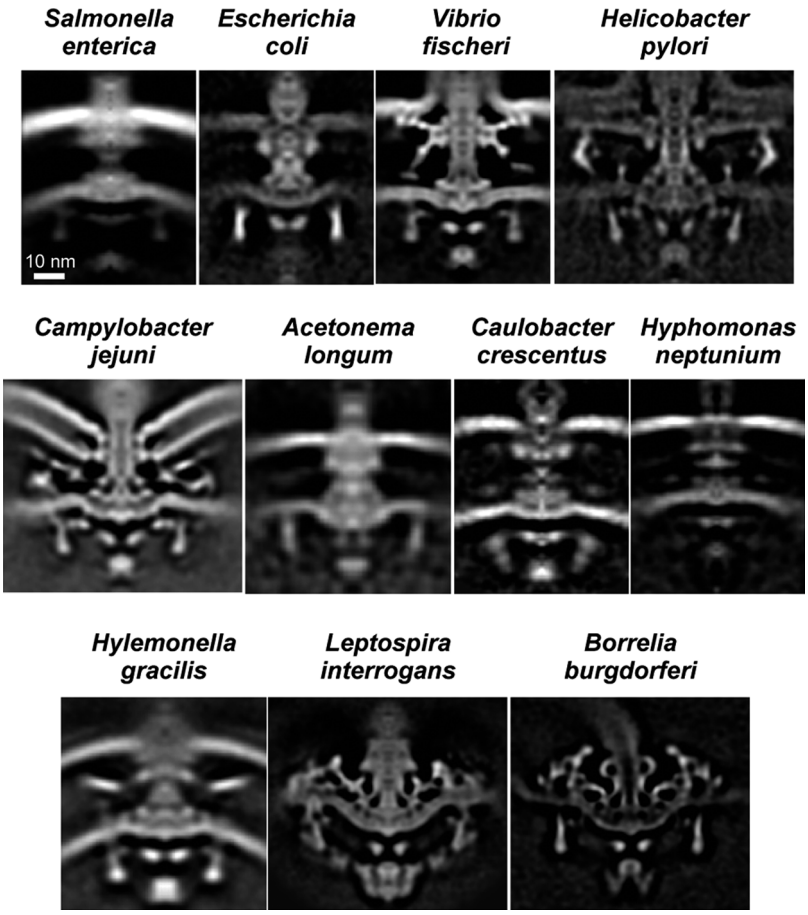

Figure 1 Structural differences in the flagellar basal body among bacterial species. *in situ* structures of the flagellar basal bodies are visualized by electron cryotomography and subtomogram averaging. The central section maps of the basal bodies of *Salmonella enterica* (EMDataBank ID: EMD-2521), *Escherichia coli* (EMDataBank ID: EMD-5311), *Vibrio fischeri* (EMDataBank ID: EMD-3155), *Helicobacter pylori* (EMDataBank ID: EMD-8459), *Campylobacter jejuni* (EMDataBank ID: EMD-3150), *Acetonema longum* (EMDataBank ID: EMD-5297), *Caulobacter crescentus* (EMDataBank ID: EMD-5312), *Hyphomonas neptunium* (EMDataBank ID: EMD-5313), *Hylemonella gracilis* (EMDataBank ID: EMD-5309), *Leptospira interrogans* (EMDataBank ID: EMD-5913) and *Borrelia burgdorferi* (EMDataBank ID: EMD-5627).

body and couple the proton flow through a proton channel with torque generation. These structures and their organization are highly conserved among bacterial species.

Electron cryotomography (ECT) is an imaging technique that directly provides 3D structure of cells and molecular complexes in their cellular environment at nanometer resolution. To obtain the structures of specimens, the specimen grid is tilted incrementally around an axis perpendicular to the electron beam, e.g. from –60° to +60° with 2° increments, and images are taken at each tilt angle. The images of a tilt series are aligned and are back-projected to generate a 3D image (tomogram) of the specimen. However, each tilt image is recorded at low electron doses to minimize radiation damage of biological samples. This leads to extremely low signal to noise ratio in each tomogram, making it necessary to align and average hundreds of particles images to increase the signal to noise ratio and to reconstruct the 3D structure at high resolution. Using this method, *in situ* structural analyses of the flagellar motors derived from different bacterial species have shown novel and divergent structures around the conserved core structure in different species (Fig. 1) [5,6].

In this review article, we describe the conserved structure of the flagellar basal body and its structural diversity.

Conserved structure of the flagellar basal body

Intact structures of the bacterial flagella derived from different bacterial species have been visualized by ECT (Fig. 1). The MS ring, the C ring, the rod and the protein export apparatus show similar structures to those of the *Salmonella* flagellar basal body (Figs. 1 and 2) [7,8]. The transmembrane protein, FliF, self-assembles into the MS ring in the cytoplasmic membrane [9]. Three cytoplasmic proteins, namely FliG, FliM and FliN, form the C ring on the cytoplasmic face of the MS ring [10]. The MS and C rings together act as a

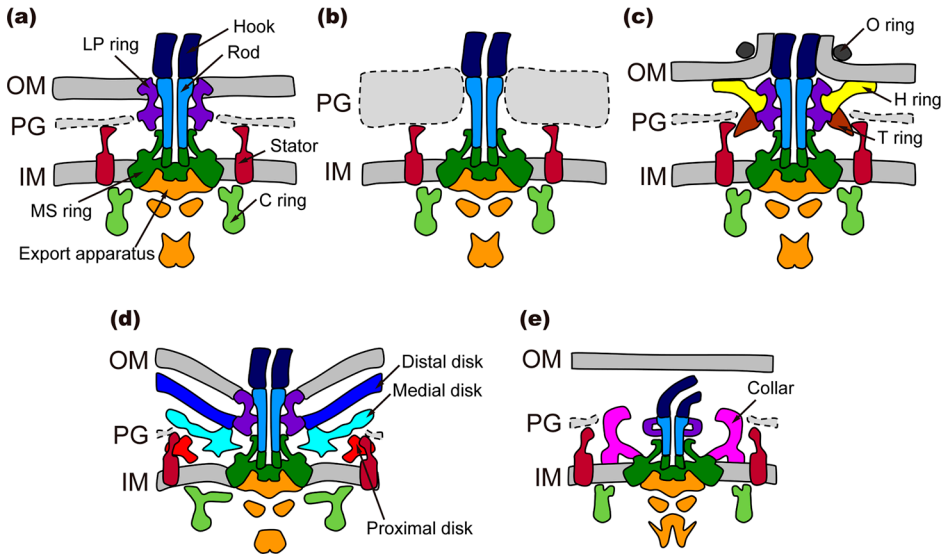

Figure 2 Cartoons of the flagellar motor derived from (a) *Salmonella*, (b) *B. subtilis*, (c) *V. alginolyticus*, (d) *C. jejuni* and (e) *B. burgdorferi*. The schematic diagrams of the *Salmonella*, *V. alginolytics*, *C. jejuni* and *B. burgdorfer* flagellar motors are shown based on their *in situ* structures whereas the *B. subtilis* motor is drawn based on purified basal body structure with some speculations. The common architectures are indicated by following colors: MS ring, green; C ring, light green; export apparatus, orange; rod, cyan; hook, navy; LP ring, purple; stator, wine red. The position of the stator unit in the *Salmonella* and *B. subtilis* motors remains unclear. The additional structures are showed in following colors: H-ring, yellow; T-ring, brown; O-ring, dark gray; basal disk, blue; median disk, light blue; proximal disk, red; P-collar, pink. IM, inner membrane; PG, peptidoglycan layer; OM, outer membrane.

rotor of the flagellar motor. The rod is composed of three distal rod proteins, FlgB, FlgC, FlgF and the distal rod protein, FlgG. The rod is a rigid, tubular structure composed of 11 protofilaments and acts as a drive shaft [11,12]. A basal body protein, FliE, which is highly conserved among bacterial species, assembles at the periplasmic surface of the MS ring to form a MS ring/rod junction zone to presumably overcome the mismatch between the rotational symmetry of the MS ring and the helical symmetry of the rod [13].

The protein export apparatus is composed of a transmembrane export gate complex made of FlhA, FlhB, FliP, FliQ, and FliR, and a cytoplasmic ATPase ring complex consisting of FliH, FliI, and FliJ [14–16]. The transmembrane protein, FliO, is required for efficient assembly of the core structure of the export gate complex made of FliP, FliQ and FliR although it is not essential for flagellar protein export [16,17]. The cytoplasmic ATPase ring complex is associated with the basal body through interactions of the extreme N-terminal region of FliH with FlhA and FliN [18–22]. The protein export apparatus utilizes ATP hydrolysis by the FliI ATPase and proton motive force across the cytoplasmic membrane as the energy sources to transport flagellar component proteins from the cytoplasm to the distal end of the growing structure where their assembly occurs [23–25].

The stator unit is composed of two transmembrane proteins, commonly referred to as MotA and MotB in the H^+-driven motor, PomA and PomB in the Na^+-driven motor of marine *Vibrio* and MotP and MotS in the Na^+-driven motor of alkalophilic *Bacillus* species. The stator unit acts as an ion channel to couple the ion flow with torque generation [26]. The MotAB and PomAB complexes are anchored to the peptidoglycan layer through a highly conserved peptidoglycan binding motif in the C-terminal periplasmic domains of MotB and PomB, respectively, thereby allowing the MotAB and PomAB complexes to act as an active H^+-type and Na^+-type stator units in the motor, respectively [27,28]. A dozen MotAB stator units surround the rotor in the *E. coli* and *Salmonella* flagellar motors. However, these stator units have not been visualized by ECT because they are not permanently fixed in place around the rotor (Fig. 1). Interestingly, the flagellar motor itself regulates the number of active stator units around the rotor in response to changes in external load and ion motive force across the cytoplasmic membrane [29–34].

LP ring complex of the flagellar basal body

FlgH and FlgI assemble around the rod in the outer membrane and the peptidoglycan layer, respectively, to form the LP ring complex, which acts as a molecular bushing [35]. In contrast to component proteins of the rod, hook and filament, FlgH and FlgI are synthesized as precursor forms with their secretion signal sequence in the cytoplasm, translocated across the cytoplasmic membrane by the Sec translocon, and subjected to signal peptide cleavage [36,37]. The LP ring complex is missing in gram-positive bacteria such as *Bacillus subtilis* (Fig. 2b) [38], suggesting that much thicker peptidoglycan layer can act as a bushing of the *Bacillus*

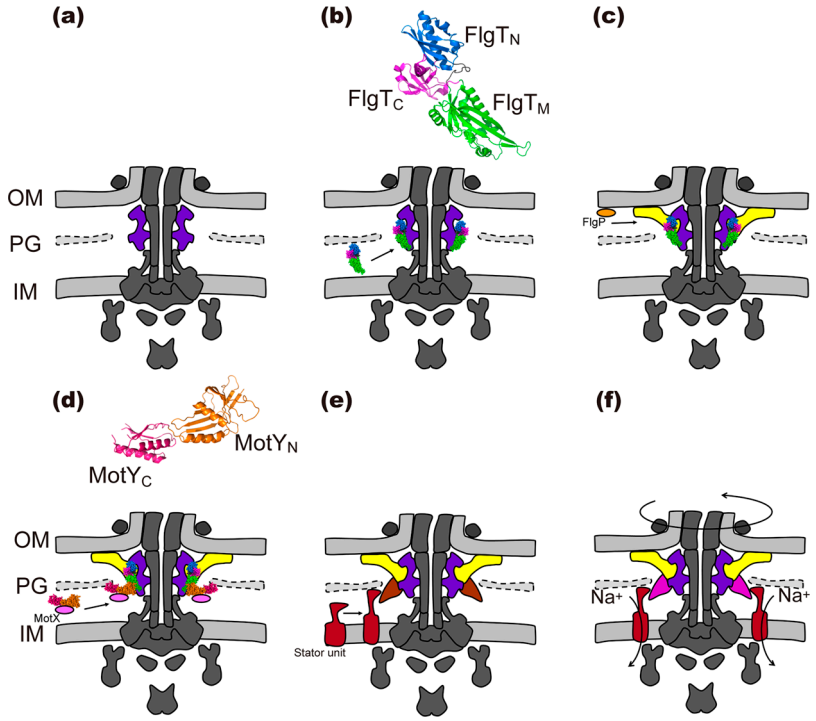

Figure 3 Assembly process of the marine *Vibrio* motor. (a) The common architecture is formed. (b) FlgT (PDB ID: 3W1E) assembles around the LP ring. (c) FlgP, which is shown by an orange ellipse, associates with $FlgT_N$ to form the H ring in the outer membrane (OM). (d) MotY (PDB ID: 2ZF8) binds to $FlgT_M$ and the PG layer, and then MotX, which is shown by a pink ellipse, interacts with MotY to form the T ring. (e) The stator units (wine red) assemble around the basal body through interactions of PomB with the PG layer and MotX. (f) The flagellar motor utilizes Na^+ as a coupling ion to drive motor rotation at the maximum speed of 1,700 revolutions per second.

flagellar motor instead of the LP ring complex.

The flagellar motor of marine *Vibrio*

The flagellar motor of *Vibrio alginolyticus* can spin at the maximum speed of 1,700 revolutions per second compared to the *Salmonella* motor, which rotates at 300 revolutions per second [39]. The marine *Vibrio* motor has two additional H and T ring structures surrounding the LP ring complex [40–43] (Fig. 2c). The H and T rings are responsible for stable anchoring of the flagellum to the cell for such a high-speed rotation [41,44]. FlgT directly binds to the basal body and promotes the formation of the T and H rings around the LP ring complex (Fig. 3) [41]. FlgT consists of three domains: $FlgT_N$, $FlgT_M$ and $FlgT_C$ (Fig. 3b) [42]. $FlgT_N$ forms an outer rim of the H ring structure made of FlgP in the outer membrane (Fig. 3c) [42,45]. Inter-subunit interactions between $FlgT_C$ domains stabilize the FlgT ring structure [42]. $FlgT_M$ is crucial for H ring formation as well as T ring formation. MotX and MotY together form the T ring with the 13-fold rotational symmetry [40,45,46]. MotY directly binds to $FlgT_M$, thereby inducing the formation of the T ring structure beneath the P ring (Fig. 3d) [40,41]. MotY consists of two domains: $MotY_N$ and $MotY_C$ (Fig. 3d) [47]. $MotY_C$ associates with the peptidoglycan layer through its peptidoglycan binding motif [47]. $MotY_N$ is responsible not only for the interaction with $FlgT_M$ but also for the interaction with MotX [40,47]. In contrast to the MotAB stator unit in the *E. coli* and *Salmonella* motors, clearly defined electron density corresponding to the PomAB stator unit has been observed by ECT [45,46]. MotX allows thirteen Na^+-type PomAB stator units to assemble into the basal body through an interaction between PomB and MotX (Fig. 3d). Since the Na^+-type PomAB stator complex cannot assemble into the *Vibrio* motor in the absence of the T ring, the T ring is responsible not only for efficient stator assembly around the rotor but also for strongly anchoring the PomAB stator to the motor, allowing the motor to spin at much higher speed up to 1,700 revolutions per second (Fig. 3e) [40,45].

The *Vibrio* flagellum is wrapped by a sheath, which is derived from the outer membrane. The outer membrane surrounds the hook and filament, thereby causing a 90° bend of the outer membrane. Recently, a new ring structure, named the O ring, has been identified around the basal body [46]. The O ring is located at the 90º bend end of the outer membrane (Fig. 2c). Since unsheathed *Vibrio* flagellum does not possess the O ring structure, the O ring may contribute to remodeling of the outer membrane for the sheath formation surrounding the hook and filament [46]. Interestingly, the LPHT quaternary ring complex shows a sliding motion along

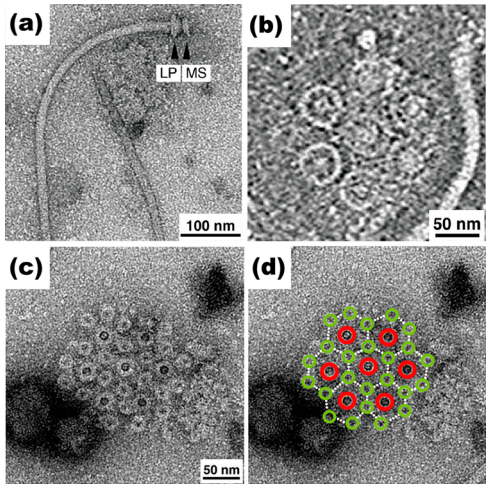

Figure 4 Flagellar structure of magnetotactic bacterium MO-1. (a) Electron micrograph of isolated flagellum with negative staining. The MS ring and the LP ring complex are shown. (b) ECT image of the flagellar basal body around the cytoplasmic membrane. (c) Negatively stained EM image of a detergent-solubilized base platform isolated from MO-1 cells. Seven flagella and twenty four fibrils together form an intertwined hexagonal array. (d) The same image as (c) with large red and small light green circles overlaid on the flagellar and fibril basal bodies, respectively.

the axial rod structure, suggesting that the friction between the rod and the inner surface of the LP ring complex is extremely small [46].

The flagellar motor of *Campylobacter jejuni*

Many of pathogenic ε-proteobacteria prefer to live in digestive tracts and hence can powerfully swim through mucous layer of the digestive tracts. In fact, *Helicobacter pylori* cells can keep swimming even under very high viscosity condition where *E. coli* cells cannot [48]. Torque generated by the flagellar motor of *H. pylori* has been estimated to be 3,600 pN nm, which is about two times higher than that by the *E. coli* motor [49]. This suggests that the flagellar motor of ε-proteobacteria has adapted to function in high viscous environments. The flagellar motor derived from *Campylobacter* and *Helicobacter* spp. possesses extensive disk structures in the periplasmic space (Fig. 1) [7]. The *C. jejuni* motor has three distinct disk-like structures: a basal disk beneath the outer membrane, a proximal disk located at a position adjacent to the cytoplasm membrane and a medial disk connecting the proximal and basal disks (Fig. 2d) [45]. Seventeen MotAB stator units have been visualized to surround the basal body [45]. FlgP forms the basal disk structure with the help of FlgQ [50]. Interestingly, there is no FlgT homologue in *C. jejuni*, suggesting that FlgP itself directly binds to the basal body. The basal disk adopts a funnel shape, and hence the outer membrane is distorted [45]. Lack of the basal disk leads to a loss of the medial and proximal disks, which are formed by PflA and PflB, respectively, suggesting that the basal disk is required for the assembly of the medial and proximal disks [45]. PflA is required for the assembly of PflB into the proximal disk. Since PflB is required for stator assembly around the rotor, these two disks presumably allow seventeen stator units to tightly associate with the motor to generate much larger torque than that of *E. coli* [45].

The flagellar motor of *Spirochete*

Spirochetes cause some serious diseases in human and animals, including leptospirosis (*Leptospira interrogans*), Lyme disease (*Borrelia burgdorferi*) and syphilis (*Treponema pallidum*). Their morphology and motility is markedly different from other bacteria. The cell shape is an elongated corkscrew that is suitable for swimming in highly viscous environments. The flagella are elongated between the outer membrane and the peptidoglycan layer and contribute to such a unique morphology of spirochetes. The flagellar motor has a bowl-like structure called "collar" that surrounds the MS ring and the rod (Figs. 1 and 2e). The collar is easily dissociated from the basal body during the purification of the hook-basal body, suggesting that it is not tightly associated with the basal body. Recently, *flbB* has been identified as a gene responsible for collar assembly [51]. FlbB is a transmembrane protein with a single N-terminal transmembrane helix and is located in the basal part of the collar structure, suggesting that FlbB anchors the collar structure to the cell membrane.

The distal rod length in spirochetes is different from that of other bacteria, such as *E. coli* and *Salmonella*. The rod length of *B. burgdorferi* is ~4 nm whereas the proximal and distal rods of *Salmonella* is 6.9 nm and 17.7 nm, respectively [12,52,53]. Since the periplasmic filament does not penetrate the outer membrane, such a shorter rod may be long enough to function as a drive shaft of the flagellar motor in *B. burgdorferi*.

The flagellar motor derived from *L. interrogans* has both the L and P rings [54] whereas the *T. pallidum* motor does not [55]. Interestingly, *B. burgdorferi* possesses only the P ring [56]. Thus, there is a clear difference in existence of the LP ring complex among the spirochetes.

The flagellar motor of marine magnetotactic bacterium MO-1

Marine magnetotactic bacterium MO-1 senses the geomagnetic direction by a unique organelle containing nanoscale magnets, namely magnetosome, and hence can orient its cell body along the geomagnetic field line. The swimming speed of MO-1 cells is up to 300 μm/sec, which is about 10-fold faster than those of *E. coli* and *Salmonella* cells. The entire architecture of the flagella isolated form the MO-1 cells look similar to that of *Salmonella* (Fig. 4a). However, the diameter of the LP ring complex is somehow

larger than that of the *Salmonella* one, raising the possibility that additional structures surround the LP ring complex in a way similar to the *Vibrio* and *Campylobacter* motors. The MO-1 cell has two highly organized flagellar bundle structures on the cell surface. Each flagellar bundle structure is composed of seven flagella and 24 fibrils in a sheath [57]. The seven flagellar filaments, which are arranged in a hexagonal array (Fig. 4b), are enveloped with 24 fibrils in the sheath (Fig. 4c, d) [57]. The basal bodies of seven flagella and 24 fibrils form intertwined hexagonal array in the cell membranes (Fig. 4d). One unit lattice is located in the center of the hexagonal array, and the other six lattices surround the center unit. Each flagellum is located at the center of each unit lattice, and six fibrils surround each flagellum in the hexagonal array. As a result, the 24 fibrils are packed together with the seven flagella in the sheath, and hence the formation of a much tighter and stronger bundle structure allows for very first swimming of MO-1 cells [57].

Conclusion

Recent structural analyses of the flagellar motors derived from different bacterial species by ECT have revealed a considerable diversity in the flagellar motor structures among bacterial species, suggesting that flagellar motors have adapted to function in the context of phylogenetically diverse bacteria. Functional and structural characterizations of the flagellar motors of different bacteria will provide insights into the evolution and function of the flagellar motor.

Acknowledgements

We gratefully thank Keiichi Namba, Michio Homma and Masahiro Ueda for continuous support and encouragement. Our research is supported in part by JSPS KAKENHI Grant Numbers JP15K14498 and JP15H05593 (to Y. V. M), JP15H02386 (to K. I.) and JP26293097 (to T. M.) and MEXT KAKENHI Grant Numbers JP26115720 and JP15H01335 (to Y. V. M) and JP24117004 and JP15H01640 (to T. M.).

Conflict of Interest

The authors declare no conflict of interests

Author Contributions

H. T., A. K., Y. V. M., K. I. and T. M. wrote the paper.

References

[1] Pallen, M. J. & Matzke, N. J. From the origin of species to the origin of bacterial flagella. *Nat. Rev. Microbiol.* **4**, 789–790 (2006).
[2] Berg, H. C. The rotary motor of bacterial flagella. *Annu. Rev. Biochem.* **72**, 19–54 (2003).
[3] Minamino, T., Imada, K. & Namba, K. Molecular motors of the bacterial flagella. *Curr. Opin. Struct. Biol.* **18**, 693–701 (2008).
[4] Terashima, H., Kojima, S. & Homma, M. Flagellar motility in bacteria: Structure and function of flagellar motor. *Int. Rev. Cell Mol. Biol.* **270**, 39–85 (2008).
[5] Zhao, X., Norris, S. J. & Liu, J. Molecular architecture of the bacterial flagellar motor in cells. *Biochemistry* **53**, 4323–4333 (2014).
[6] Minamino, T. & Imada, K. The bacterial flagellar motor and its structural diversity. *Trends Microbiol.* **23**, 267–274 (2015).
[7] Chen, S., Beeby, M., Murphy, G. E., Leadbetter, J. R., Hendrixson, D. R., Briegel, A., *et al.* Structural diversity of bacterial flagellar motors. *EMBO J.* **30**, 2972–2981 (2011).
[8] Kawamoto, A., Morimoto, Y. V., Miyata, T., Minamino, T., Hughes, K. T., Kato, T., *et al.* Common and distinct structural features of *Salmonella* injectisome and flagellar basal body. *Sci. Rep.* **3**, 3369 (2013).
[9] Ueno, T., Oosawa, K. & Aizawa, S. M ring, S ring and proximal rod of the flagellar basal body of *Salmonella typhimurium* are composed of subunits of a single protein, FliF. *J. Mol. Biol.* **227**, 672–677 (1992).
[10] Khan, I. H., Reese, T. S. & Khan, S. The cytoplasmic component of the bacterial flagellar motor. *Proc. Natl. Acad. Sci. USA* **89**, 5956–5960 (1992).
[11] Homma, M., Kutsukake, K., Hasebe, M., Iino, T. & Macnab, R. M. FlgB, FlgC, FlgF and FlgG. A family of structurally related proteins in the flagellar basal body of *Salmonella typhimurium*. *J. Mol. Biol.* **211**, 465–477 (1990).
[12] Fujii, T., Kato, T., Hiraoka, D., Miyata, T., Minamino, T., Chevance, F., *et al.* Identical folds used for distinct mechanical functions of the bacterial flagellar rod and hook. *Nat. Commun.* **8**, 14276 (2017).
[13] Minamino, T., Yamaguchi, S. & Macnab, R.M. Interaction between FliE and FlgB, a proximal rod component of the flagellar basal body of *Salmonella*. *J. Bacteriol.* **182**, 3029–3036 (2000).
[14] Minamino, T. & Macnab, R. M. Components of the *Salmonella* flagellar export apparatus and classification of export substrates. *J. Bacteriol.* **181**, 1388–1394 (1999).
[15] Minamino, T. & Macnab, R. M. Interactions among components of the *Salmonella* flagellar export apparatus and its substrates. *Mol. Microbiol.* **35**, 1052–1064 (2000).
[16] Fukumura, T., Makino, F., Dietsche, T., Kinoshita, M., Kato, T., Wagner, S., *et al.* Assembly and stoichiometry of the core structure of the bacterial flagellar type III export gate complex. *PLoS Biol.* **15**, e2002281 (2017).
[17] Fabiani, F. D., Renault, T. T., Peters, B., Dietsche, T., Gálvez, E. J. C., Guse, A., *et al.* A flagellum-specific chaperone facilitates assembly of the core type III export apparatus of the bacterial flagellum. *PLoS Biol.* **15**, e2002267 (2017).
[18] González-Pedrajo, B., Minamino, T., Kihara, M. & Namba, K. Interactions between C ring proteins and export apparatus components: a possible mechanism for facilitating type III protein export. *Mol. Microbiol.* **60**, 984–998 (2006).
[19] Minamino, T., Yoshimura, S. D. J., Morimoto, Y. V., González-Pedrajo, B., Kami-ike, N. & Namba, K. Roles of the extreme N-terminal region of FliH for efficient localization of the FliH-FliI complex to the bacterial flagellar type III export apparatus. *Mol. Microbiol.* **74**, 1471–1483 (2009).
[20] Hara, N., Morimoto, Y. V., Kawamoto, A., Namba, K. & Minamino, T. Interaction of the extreme N-terminal region of FliH with FlhA is required for efficient bacterial flagellar protein export. *J. Bacteriol.* **194**, 5353–5360 (2012).
[21] Bai, F., Morimoto, Y. V., Yoshimura, S. D. J., Hara, N., Kami-ike, N., Namba, K., *et al.* Assembly dynamics and the roles of FliI ATPase of the bacterial flagellar export apparatus.

Sci. Rep. **4**, 6528 (2014).
[22] Notti, R. Q., Bhattacharya, S., Lilic, M. & Stebbins, C. E. A common assembly module in injectisome and flagellar type III secretion sorting platforms. *Nat. Commun*. **6**, 7125 (2015).
[23] Minamino, T. & Namba, K. Distinct roles of the FliI ATPase and proton motive force in bacterial flagellar protein export. *Nature* **451**, 485–488 (2008).
[24] Paul, K., Erhardt, M., Hirano, T., Blair, D. F. & Hughes, K. T. Energy source of the flagellar type III secretion. *Nature* **451**, 489–492 (2008).
[25] Minamino, T., Morimoto, Y. V., Hara, N. & Namba, K. An energy transduction mechanism used in bacterial flagellar type III protein export. *Nat. Commun.* **2**, 475 (2011).
[26] Morimoto, Y. V. & Minamino, T. Structure and function of the bi-directional bacterial flagellar motor. *Biomolecules* **4**, 217–234 (2014).
[27] Kojima, S., Imada, K., Sakuma, M., Sudo, Y., Kojima, C., Minamino, T., *et al.* Stator assembly and activation mechanism of the flagellar motor by the periplasmic region of MotB. *Mol. Microbiol.* **73**, 710–718 (2009).
[28] Zhu, S., Takao, M., Li, N., Sakuma, M., Nishino, Y., Homma, M., *et al.* Conformational change in the periplasmic region of the flagellar stator complex coupled with the assembly around the rotor. *Proc. Natl. Acad. Sci. USA* **111**, 13523–13528 (2014).
[29] Fukuoka, H., Wada, T., Kojima, S., Ishijima, A. & Homma, M. Sodium-dependent dynamic assembly of membrane complexes in sodium-driven flagellar motors. *Mol. Microbiol.* **71**, 825–835 (2009).
[30] Lele, P. P., Hosu, B. G. & Berg, H. C. Dynamics of mechanosensing in the bacterial flagellar motor. *Proc. Natl. Acad. Sci. USA* **110**, 11839–11844 (2013).
[31] Tipping, M. J., Steel, B. C., Delalez, N. J., Berry, R. M. & Armitage, J. P. Quantification of flagellar motor stator dynamics through *in vivo* proton-motive force control. *Mol. Microbiol.* **87**, 338–347 (2013).
[32] Che, Y. S., Nakamura, S., Morimoto, Y. V., Kami-ike, N., Namba, K. & Minamino, T. Load-sensitive coupling of proton translocation and torque generation in the bacterial flagellar motor. *Mol. Microbiol.* **91**, 175–184 (2014).
[33] Castillo, D. J., Nakamura, S., Morimoto, Y. V., Che, Y. S., Kami-ike, N., Kudo, S., *et al.* The C-terminal periplasmic domain of MotB is responsible for load-dependent control of the number of stators of the bacterial flagellar motor. *Biophysics* **9**, 173–181 (2013).
[34] Terahara, N., Noguchi, Y., Nakamura, S., Kami-ike, N., Ito, M., Namba, K., *et al.* Load- and polysaccharide-dependent activation of the Na^+-type MotPS stator in the *Bacillus subtilis* flagellar motor. *Sci. Rep.* **7**, 46081 (2017).
[35] Akiba, T., Yoshimura, H. & Namba, K. Monolayer crystallization of flagellar L-P rings by sequential addition and depletion of lipid. *Science* **252**, 1544–1546 (1991).
[36] Homma, M., Komeda, Y., Iino, T. & Macnab, R. M. The *flaFIX* gene product of *Salmonella typhimurium* is a flagellar basal body component with a signal peptide for export. *J. Bacteriol.* **169**, 1493–1498 (1987).
[37] Jones, C. J., Homma, M. & Macnab, R. M. Identification of proteins of the outer (L and P) rings of the flagellar basal body of *Escherichia coli*. *J. Bacteriol.* **169**, 1489–1492 (1987).
[38] Kubori, T., Okumura, M., Kobayashi, N., Nakamura, D., Iwakura, M. & Aizawa, S. Purification and characterization of the flagellar hook-basal body complex of *Bacillus subtilis*. *Mol. Microbiol.* **24**, 399–410 (1997).
[39] Magariyama, Y., Sugiyama, S., Muramoto, K., Maekawa, Y., Kawagishi, I., Imae, Y., *et al.* Very fast flagellar rotation. *Nature* **371**, 752 (1994).
[40] Terashima, H., Fukuoka, H., Yakushi, T., Kojima, S. & Homma, M. The *Vibrio* motor proteins, MotX and MotY, are associated with the basal body of Na-driven flagella and required for stator formation. *Mol. Microbiol.* **62**, 1170–1180 (2006).
[41] Terashima, H., Koike, M., Kojima, S. & Homma, M. The flagellar basal body-associated protein FlgT is essential for a novel ring structure in the sodium-driven *Vibrio* motor. *J. Bacteriol.* **192**, 5609–5615 (2010).
[42] Terashima, H., Li, N., Sakuma, M., Koike, M., Kojima, S., Homma, M., *et al.* Insight into the assembly mechanism in the supramolecular rings of the sodium-driven *Vibrio* flagellar motor from the structure of FlgT. *Proc. Natl. Acad. Sci. USA* **110**, 6133–6138 (2013).
[43] Hosogi, N., Shigematsu, H., Terashima, H., Homma, M. & Nagayama, K. Zernike phase contrast cryo-electron tomography of sodium-driven flagellar hook-basal bodies from *Vibrio alginolyticus*. *J. Struct. Biol.* **173**, 67–76 (2011).
[44] Martinez, R. M., Jude, B. A., Kirn, T. J., Skorupski, K. & Taylor R. K. Role of FlgT in anchoring the flagellum of Vibrio cholerae. *J. Bacteriol.* **192**, 2085–2092 (2010).
[45] Beeby, M., Ribardo, D. A., Brennan, C. A., Ruby, E. G., Jensen, G. J. & Hendrixson, D. R. Diverse high-torque bacterial flagellar motors assemble wider stator rings using a conserved protein scaffold. *Proc. Natl. Acad. Sci. USA* **113**, E1917–E1926 (2016).
[46] Zhu, S., Nishikino, T., Hu, B., Kojima, S., Homma, M. & Liu, J. Molecular architecture of the sheathed polar flagellum in *Vibrio alginolyticus*. *Proc. Natl. Acad. Sci. USA* **114**, 10966–10971 (2017).
[47] Kojima, S., Shinohara, A., Terashima, H., Yakushi, T., Sakuma, M., Homma, M., *et al.* Insights into the stator assembly of the *Vibrio* flagellar motor from the crystal structure of MotY. *Proc. Natl. Acad. Sci. USA* **105**, 7696–7701 (2008).
[48] Hazell, S. L., Lee, A., Brady, L. & Hennessy, W. *Campylobacter pyloridis* and *gastritis*: association with intercellular spaces and adaptation to an environment of mucus as important factors in colonization of the gastric epithelium. *J. Infect. Dis.* **153**, 658–663 (1986).
[49] Celli, J. P., Turner, B. S., Afdhal, N. H., Keates, S., Ghiran, I., Kelly, C. P., *et al. Helicobacter pylori* moves through mucus by reducing mucin viscoelasticity. *Proc. Natl. Acad. Sci. USA* **106**, 14321–14326 (2009).
[50] Sommerlad, S. M. & Hendrixson, D. R. Analysis of the roles of FlgP and FlgQ in flagellar motility of *Campylobacter jejuni*. *J. Bacteriol.* **189**, 179–186 (2007).
[51] Moon, K. H., Zhao, X., Manne, A., Wang, J., Yu, Z., Liu, J., *et al.* Spirochetes flagellar collar protein FlbB has astounding effects in orientation of periplasmic flagella, bacterial shape, motility, and assembly of motors in *Borrelia burgdorferi*. *Mol. Microbiol.* **102**, 336–348 (2016).
[52] Zhao, X., Zhang, K., Boquoi, T., Hu, B., Motaleb, M. A., Miller, K. A., *et al.* Cryoelectron tomography reveals the sequential assembly of bacterial flagella in *Borrelia burgdorferi*. *Proc. Natl. Acad. Sci. USA* **110**, 14390–14395 (2013).
[53] Jones, C. J., Macnab, R. M., Okino, H. & Aizawa, S. Stoichiometric analysis of the flagellar hook-(basal-body) complex of *Salmonella typhimurium*. *J. Mol. Biol.* **212**, 377–387 (1990).
[54] Raddi, G., Morado, D. R., Yan, J., Haake, D. A., Yang, X. F. & Liu, J. Three-dimensional structures of pathogenic and saprophytic *Leptospira* species revealed by cryo-electron tomography. *J. Bacteriol.* **194**, 1299–1306 (2012).
[55] Liu, J., Howell, J. K., Bradley, S. D., Zheng, Y., Zhou, Z. H. & Norris, S. J. Cellular architecture of *Treponema pallidum*: novel flagellum, periplasmic cone, and cell envelope as revealed by cryo electron tomography. *J. Mol. Biol.* **403**, 546–561 (2010).

[56] Liu, J., Lin, T., Botkin, D J., McCrum, E., Winkler, H. & Norris, S. J. Intact flagellar motor of *Borrelia burgdorferi* revealed by cryo-electron tomography: evidence for stator ring curvature and rotor/C-ring assembly flexion. *J. Bacteriol.* **191**, 5026–5036 (2009).
[57] Ruan, J., Kato, T., Santini, C. L., Miyata, T., Kawamoto, A., Zhang, W. J., *et al.* Architecture of a flagellar apparatus in the fast-swimming magnetotactic bacterium MO-1. *Proc. Natl. Acad. Sci. USA* **109**, 20643–20648 (2012).